Bulletin of the New Zealand Society for Earthquake Engineering, Vol. 51, No. 2, June 2018

EXPERIMENTAL IN-PLANE PERFORMANCE OF INSULATED CONCRETE AND BRICK MASONRY WALL PANELS RETROFITTED USING POLYMER COMPOSITES

Najif Ismail[1], Tamer El-Maaddawy[2], Amanullah Najmal[3] and Nouman Khattak[4]

(Submitted *March 2017*; Reviewed *July 2017*; Accepted *November 2017*)

ABSTRACT

Masonry infilled reinforced concrete frame buildings built prior to the introduction of modern seismic provisions have been observed to undergo damage in and around the masonry infill walls during most recent moderate to severe earthquakes. Fibre reinforced cementitious matrix (FRCM) is one of several retrofitting options available to limit such earthquake induced damage to infill walls. An experimental program was undertaken herein to experimentally investigate the effectiveness of FRCM as a strengthening solution for vintage (i.e. built between 1880 and 1930) un-reinforced brick masonry (URM) and insulated concrete masonry (IMU) infill walls. A total of 16 masonry assemblages were tested under in-plane diagonal load, of these 8 were constructed replicating vintage URM whereas the remainder were constructed using modern IMU. IMU is a preferred masonry type in hot and humid regions owing to its superior insulting capability. Different polymer fabrics (i.e., carbon, glass and basalt) were applied over both faces of test walls, with two replicate test walls receiving the same FRCM strengthening details. One test wall of each masonry type was tested as-built to serve as a control specimen for comparison. One wall of each masonry type received two layers of basalt FRCM. The investigated aspects included stress-strain behaviour, stiffness, and ductility. Shear strength increment observed due to single layer of FRCM application was 422-778% for vintage URM and 307-415% for modern IMU. FRCM also substantially increased the ductility capacity of the masonry assemblages.

INTRODUCTION

Masonry infilled reinforced concrete frame (MIF) is one of the widely used lateral resisting systems in the Middle East and Asia, while several potentially earthquake-prone MIF buildings (mainly built prior to the introduction of seismic design concepts in 1960s) also prevail in Europe, New Zealand, and US. A notable population of pre-1960s MIF buildings also prevail in New Zealand [1], which were mainly designed to take gravity loading only and have small column dimensions (referred to as vintage buildings hereafter). Structural contribution of masonry infills towards building stiffness and strength is often neglected in assessment and design, although it is now widely recognised that infill walls have significant effect on building's global and local earthquake performance. It is also widely accepted that the interaction of masonry infill walls and the surrounding frame is rather complex and warrants careful consideration during the design and evaluation [2]. Such MIF evaluation requires accurate behavioural models for all structural elements, including that for infill masonry walls.

MIF buildings have been observed to undergo damage during almost all past large earthquakes such as 2008 Wenchuan earthquake [3], 2011 Christchurch earthquakes [4], 2015 Hindu Kush earthquake [5], and 2016 Gorkha earthquake [6]. It had been reported that at several instances damage to non-structural components such as stairways, ceilings, partition walls, and infill masonry panels restricted the use of the building, even when structural damage was limited or negligible. Furthermore, damaged infill walls further pose a safety risk to passer-by. One option to alleviate this problem is the introduction of a strengthening technique that can delay the onset of cracking and increase the deformation capacity. Infill masonry walls may experience two type of loading during an earthquake depending upon their orientation with respect to the principal direction of earthquake excitation: in-plane loads and/or face loads leading to out-of-plane collapse. The commonly observed in-plane failure modes include sliding along mortar bed joints, diagonal cracking through masonry units, step mortar joint sliding/cracking, and/or toe crushing. Typical failure modes widely accepted for masonry infills are shown graphically in Figure 1.

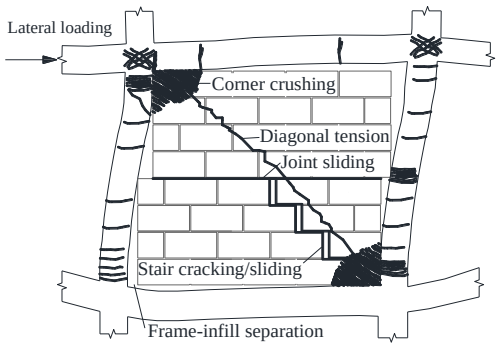

Figure 1. Typical masonry infill wall failure modes

Masonry type used to construct infill panels in MIF buildings varies widely depending upon their location and year of construction. Two types of masonry were tested in this study. The first, unreinforced solid brick masonry (URM) that replicate masonry used to infill openings in vintage MIF

[1] *Corresponding Author, Lecturer, Wellington Institute of Technology, Lower Hutt, New Zealand, najif.ismail@weltec.ac.nz (Member)*
[2] *Associate Professor, United Arab Emirates University, Al Ain (UAE), tamer.maaddawy@uaeu.ac.ae*
[3] *Graduate Student, United Arab Emirates University, Al Ain (UAE), 201470422@uaeu.ac.ae*
[4] *Research Assistant, United Arab Emirates University, Al Ain (UAE), nouman@uaeu.ac.ae*

buildings i.e. those built prior to the introduction of seismic resistant provisions. The second type of masonry tested was insulated concrete masonry (IMU), which has been widely used in modern MIF buildings located in regions with hot climate owing to its perceived thermal insulating properties. The masonry test panels were constructed to replicate constituent material properties and construction details typically found in existing buildings. Figure 2a shows an IMU unit, and Figures 2b and 2c show photographs of an IMU panel and a URM test panel, respectively.

(a) IMU unit

(b) IMU test wall (c) URM test wall

Figure 2: Photos of test wall panels

The investigated seismic strengthening technique involves surface application of a polymer grid pattern fabric to the masonry substrate using an in-organic (cementitious) matrix. This technique is typically referred to as fabric reinforced cementitious matrix (FRCM) that differs from conventional FRP sheet applications in terms of binding matrix. A review of literature on FRCM strengthened masonry walls has been reported by [7], whereas a synopsis of literature on FRCM strengthened reinforced concrete elements has been compiled and reported by [8]. For brevity, only literature on in-plane shear testing of masonry panels strengthened using FRCM is discussed herein.

Yardim and Lalaj [9] tested 12 masonry panels strengthened using ferrocement, polypropylene FRCM, and glass FRCM applied on one face and both faces of test panels. Contrary to other studies, test panels with two-face FRCM application were reported to result in smaller increase in shear modulus and shear strength but with large increase in deformation capacity. All single face FRCM strengthened test panels were reported to undergo out-of-plane deformation causing large crack openings on un-strengthened face, which was similar to failure mode reported by Ismail and Ingham [10].

Ismail and Ingham [10] investigated diagonal shear behaviour of in-plane loaded vintage URM panels retrofitted using two types of FRCM systems by subjecting a total of 12 two leaf thick URM panels, of these two were tested as built and the remainder were tested after FRCM retrofitting. In-plane shear strength increase due to one-layer single sided FRCM application was reported to be 14-48 %, whereas one layer FRCM on both faces resulted in a shear strength increase of 346-381%. However, it was noted that the reported in-plane shear strength increase for single sided FRCM strengthening was conservative and corresponds to a limit state when testing was stopped due to excessive out-of-plane tilting.

Babaeidarabad et al. [11] tested nine masonry panels strengthened using carbon FRCM in induced diagonal shear failure mode. Two FRCM strengthening schemes were used, namely one and four fabric layers applied onto both faces. The average shear strength of FRCM strengthened test panels with one layer FRCM and four layer FRCM was observed to be 2.4 and 4.7 times the strength of the as-built tested URM panel respectively. It was concluded that FRCM strengthening is an effective solution to increase stiffness and pseudo-ductility of masonry panels. Babaeidarabad et al. [12] investigated the in-plane shear strength of nine unreinforced hollow concrete masonry panels strengthened using carbon FRCM. FRCM strengthened test panels exhibited a shear strength of 2.0-2.4 times that of the corresponding as-built tested panel. Sagar et al. [13] conducted an experimental study to assess the feasibility of using FRCM for strengthening of masonry panels by undertaking monotonic diagonal shear testing of small scale masonry panels (352×345 mm^2) strengthened using one-sided FRCM application. A shear strength increase of only 10 % was however reported.

Experimental performance of as-built and FRCM strengthened in-plane loaded URM and IMU wall panels was investigated herein. It is noted that minimal experimental results exist in technical literature on FRCM strengthened URM walls and no technical study has yet studied in-plane behaviour of FRCM strengthened IMU walls despite its presence in existing building stock. The presented experimental results demonstrate the effectiveness of FRCM as a strengthening solution for infill walls. The presented experimental data provides useful information for use in the design of FRCM strengthening techniques.

EXPERIMENTAL PROGRAM

A total of 16 masonry wall panels were constructed and tested under diagonal in-plane loading. The experimental program was divided into two series, with series 1 involving testing of eight URM wall panels and series 2 involving testing of 8 IMU wall panels. One wall panel from each series was tested as-built without retrofit, while the rest of the wall panels were strengthened using three different types of FRCM that included basalt, carbon and glass. A single layer of each FRCM type was applied on both faces of two replicate test walls. Additionally, one test wall of each type of masonry was strengthened with two layers of basalt FRCM on both faces to investigate the effect of double layered basalt FRCM.

Wall Specimens

Two different masonry types were used, 200 mm thick IMU and 220 mm thick URM. All masonry test walls were approximately 1.2 m^2 in size.

IMU test walls were constructed using typical construction practices adopted in the Asia and the Middle East. URM test walls were constructed to replicate masonry prevalent in pre-1960s MIF buildings in New Zealand. The bricks used to construct URM were 65×108×220 mm^3 and IMU units were 200×200×400 mm^3 (with 50 mm thick EPS core) in size. URM test walls were constructed following a common bond pattern with roughly 15-20 mm thick mortar courses, with one header course after every three stretcher courses. IMU test walls

followed a staggered stack bond pattern. Thickness of mortar head and bed joints was kept to roughly 10 mm. Each test was given a notation WX-A-N or WX-T-N, where W denotes wall, X represents test series (1 for URM walls and 2 for IMU walls), A denotes as-built specimen, T represents FRCM type (C for carbon, G for glass, and B for basalt), and N at the end denotes the test number.

Material Properties

Two different type of masonry mortar was used to construct the test walls. A cement-sand mortar with a mass ratio of 1:3 was used in the construction of IMU and a hydraulic ASTM type O mortar with a by volume composition of 1:2:9 (cement:lime:sand) was used to construct URM test walls. The mortar composition was based on findings by Lumantarna et al. [14], they have indicated that the mortar composition used in general matched the physical, chemical, and mechanical characteristics of the masonry mortar typically found in buildings built in early 19th century and thus represents the lower bound mortar strength/stiffness expected in vintage MIF buildings. It is noted that the representative bricks used in the experimental study exhibited low compressive strength in New Zealand context. However, the shear failure mode of masonry was governed by the strength of the weaker plane, which in this case was mortar and therefore the results of this experimental study are still deemed relevant to New Zealand URM buildings. Mechanical properties of each masonry type were determined experimentally and have been reported in Table 1, with associated percentage coefficient of variation (CoV). The compressive strength of masonry units was determined in accordance with ASTM C270 [15] and the mortar compressive strength was determined by testing five replicate mortar cubes (50 mm^3 in size) in accordance with ASTM C109 [16]. The compressive strength of IMU units has been calculated based on gross area of the units and is governed by splitting strength.

Table 1: Properties of masonry materials.

Test Series	Masonry Type	f'_b (MPa)		f'_j (MPa)		f_m* (MPa)	E_m** (MPa)
		Mean	CoV	Mean	CoV		
1	URM	5.7	2.6	1.5	3.4	2.9	2030
2	IMU	3.0	1.0	2.9	2.9	3.6	3240

Where: f'_b = brick/block compressive strength; CoV = coefficient of variation (%); f'_j = mortar compressive strength; f'_m= masonry compressive strength; and E_m = masonry modulus of elasticity.*calculated as $f'_m=k\, f'^{\alpha}_b\, f'^{\beta}_j$, where $\alpha = 0.7$, $\beta = 0.3$ and $k = 0.45$ for brick masonry or 0.55 for concrete masonry [17] **$E_m=700f'_m$ for clay masonry and $E_m=900f'_m$ for concrete masonry [18].

Table 2: Indicative physical characteristics of polymer fabrics used in FRCM.

Fabric Type	ρ_f	ρ_m	t_r	F_t	ε_u	E_f	*f'_{cj} (MPa)	
	(g/m^2)	(g/cm^3)	(mm)	(kN/m)	(%)	(GPa)	Mean	CoV
Glass	420	2.50	0.09	105	4.0	32	40.0	4.9
Carbon	>170	1.83	0.05	240	2.0	252	50.9	1.7
Basalt	250	2.75	0.04	60	1.8	89	38.5	5.5

Where: ρ_f = density of fabric in g/m^2; ρ_m = density of fibre; t_r = approximate thickness of a fabric roving; F_t= tensile strength of fibre grid per running meter; ε_u= rupture strain of the fabric; E_f= fabric modulus of elasticity; f'_{cj} = compressive strength of FRCM matrix; and CoV = coefficient of variation (%). *values attained by testing cubes of matrix

Three different types of FRCM systems were used to strengthen the test panels, with each FRCM system consisting of a polymer fabric and a cementitious matrix. The FRCM fabrics used herein included glass fibre reinforced polymer (glass), carbon fibre reinforced polymer (carbon) and basalt. Experimentally determined compressive strength of FRCM matrices and indicative characteristics of FRCM fabrics based on manufacturer's technical literature are reported in Table 2. The substrate - FCRM bond strength was not determined, however the FRCM manufacturer's technical datasheet shows an adhesion value of more than 2 MPa. Typically, three cubes were casted from each batch of prepared FRCM matrix, which were later tested for compression strength in accordance with ASTM C109 [16]. It is also noted that the matrix-fabric interface is usually weaker than the FRCM-substrate interface.

FRCM Application

After curing test walls for 28 days, both faces of the test walls were cleaned to remove any oil, residue, dust, or lose masonry fragments. The substrate surface of the masonry assemblages was brought to touch dry saturated condition.

a) matrix application b) fabric introduction

c) fabric overlap d) finished test wall

e) application of FRCM in a URM building in Auckland

Figure 3: FRCM strengthening of test walls.

The FRCM matrix (Planitop HDM Maxi) was prepared by mixing two-components (component-A was powder and component-B was liquid) in a pan mixer for 5 minutes. The matrix derives strength from pozzolonic reaction and contained

fine-grained aggregates, special admixtures and synthetic polymers. Freshly prepared FRCM matrix was applied onto full surface of test walls (see Figure 3a) using a flat metal trowel, by keeping a uniform thickness of 3-5 mm. The reinforcement fabric was lightly pressed into the freshly applied matrix layer (see Figure 3b). The horizontal fabric rovings were kept parallel to the direction of masonry bed joints. Over this the final finishing matrix layer was applied (see Figure 3c) and the surface was trowelled to ensure a consistent thickness. Total thickness of the FRCM overlay was kept approximately 8-15 mm. As the FRCM fabric comes with a fixed width of 0.9 m, its application on different structures would require lap splicing. In this study, an overlap of 152 mm (as suggested by ACI-549.4 [19] was used. Two specimens were provided with two layers of basalt fabric to see the effect of double layer of FRCM. Test walls were left for curing for 28 days in ambient conditions prior to testing. A finished FRCM strengthened test wall is shown in Figure 3d. Shown also is a photo in Figure 3e showing the FRCM being applied to a heritage URM building located in Auckland.

Test Setup and Instrumentation

Seismic assessment of MIF buildings requires more reliable evaluation of the in-plane shear behaviour of masonry infill walls. For this purpose, a diagonal compression test can be undertaken in accordance with ATM E519 [20], where a square masonry wall/panel with its diagonal oriented in the gravity direction is loaded along the diagonal. The test allows inducing an in-plane failure mode.

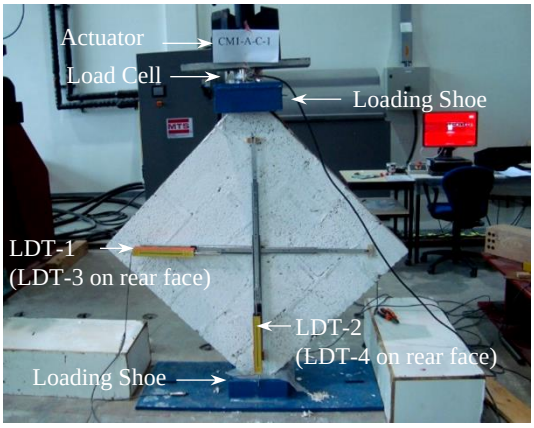

a) diagonal orientation

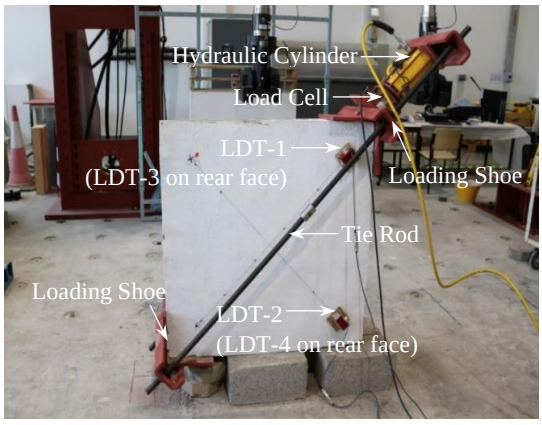

b) horizontal orientation

Figure 4: Test Setup and Instrumentation.

A modified test setup is also used for relatively weaker historic URM, in which the test wall is tested in horizontal orientation and a diagonal load is applied by wedging a hydraulic cylinder-load cell assembly between the loading shoe and a backing beam/channel connected to the other diagonal end with a set of two tie rods. Both of these two test setups were used in this study, where only the as-built IMU specimen was tested in diagonal orientation (see Figure 4a), whereas all other test panels were tested using the modified test setup shown in Figure 4b. Test panels are subjected to a displacement controlled monotonic loading gradually increasing at a rate of 0.01 mm/s. The applied diagonal load was measured using a 500 kN load cell. Resulting deformation along both diagonals of the test panel (i.e. primary and secondary deformations) were recorded using four linear displacement transducers (LDTs) mounted directly onto test walls over a gauge length of about 1200 mm.

TEST RESULTS AND DISCUSSIONS

A summary of test results is given in Table 3. Shear stress of tested panels was calculated using Equation 1, where υ is the calculated shear stress on net area, P is the recorded applied diagonal force, and A_n is the net shear plane area of test panels in mm^2. Measured strain values (ε) were calculated using Equation 2, where Δ_S is diagonal shortening of masonry along the applied force, Δ_L is diagonal elongation of masonry measured perpendicular to the applied force, and g is the gauge length of the displacement transducer.

$$\upsilon = \frac{0.707P}{A_n} \quad (1)$$

$$\varepsilon = \frac{(\Delta_S + \Delta_L)}{2g} \quad (2)$$

Experimentally calculated maximum shear strength values of all FRCM strengthened test panels were also expressed as ratio to the calculated shear strength of the corresponding as-built test panel (υ_o).

Pseudo-ductility and Toughness

Ductility may be defined as the ability of a structure to deform and yield in-elastically without experiencing a significant loss of load resistance, whereas toughness quantifies the non-hysteretic energy dissipated by a structure until failure. These are essential characteristics when seismic resistance of structures is of interest. To determine pseudo-ductility and non-hysteretic energy dissipation, an elasto-plastic idealisation was used to determine the yield strain (ε_y) and the ultimate strain (ε_u) from the experimentally obtained stress-strain curves. The two benchmark strain values were taken as the values corresponding to the shear stress values of $0.7\upsilon_{max}$ (pre-peak) and $0.80\upsilon_{max}$ (post-peak), respectively. The pseudo-ductility was calculated as the ratio of ultimate strain to yield strain i.e. $\mu = \frac{\varepsilon_u}{\varepsilon_y}$. Toughness (T) was calculated as the area under the stress-strain curve. It was evident that the FRCM strengthened test walls failed in a more ductile manner and exhibited much larger ductility and toughness when compared to as-built tested walls.

Stiffness/Modulus of Rigidity

The modulus of rigidity or shear modulus (G) for each test wall was determined as the secant modulus between the points corresponding to shear stress values of $0.1\upsilon_{max}$ and $0.7\upsilon_{max}$ on the shear stress-strain plots [7], to quantify stiffness. Elastic moduli (E) were also calculated as $E = 2G(1 + p)$, where p is the Poisson's ratio and was set to 0.25. FRCM strengthened test walls showed an elastic modulus larger than their counterpart as-built test walls, suggesting that the strengthening had increased the stiffness of test walls. The carbon FRCM strengthened test walls had the largest shear modulus and basalt

FRCM resulted in the least shear modulus, with shear modulus of glass FRCM strengthened test walls in between these two extremes. The shear moduli were observed to vary largely and are deemed not suitable to infer a definitive conclusion. The observed large variation in stiffness characteristics experimentally determined using diagonal shear testing had also been reported in technical literature e.g. [21,22], which is attributed to stress re-distribution in pre-peak range owing to masonry materials being highly heterogeneous.

Table 3: Testing details and results.

Test Panel	w (mm)	h (mm)	t (mm)	t_f (mm)	FT	NL	P_{max} (kN)	υ_{max} (MPa)	$\upsilon_{max}/\upsilon_o$	ε_y (με)	ε_u (με)	μ	T (J/m^3)	G (GPa)	E (GPa)
W1-A-1	1030	1050	220	-	-	-	31	0.09	1.00	2.34	2.34	1.0	141	0.09	0.04
W2-A-2	1040	1060	200	-	-	-	81	0.27	1.00	0.30	0.30	1.0	40	2.25	0.9
W1-G-3	1040	1055	240	10	G	1	195	0.55	6.11	0.280	11.2	40	7230	29.03	72.5
W1-G-4	1040	1055	240	10	G	1	249	0.70	7.78	0.330	3.68	11.1	3050	22.14	55.34
W1-C-5	1035	1050	245	9	C	1	134	0.38	4.22	0.138	6.20	41.9	2280	67.93	169.8
W1-C-6	1040	1055	242	9	C	1	176	0.49	5.44	0.330	7.10	21.5	3060	33.45	83.62
W1-B-7	1030	1050	235	8	B	1	183	0.53	5.89	0.228	11.2	40	5225	1.67	4.18
W1-B-8	1040	1070	242	9	B	1	223	0.62	6.89	0.223	10.0	44.8	6049	1.89	4.70
W1-B-9*	1030	1050	250	20	B	2	273	0.74	8.22	0.680	-	-	746	12.69	31.73
W2-G-10	1040	1070	220	10	G	1	310	0.96	3.56	0.210	12.0	57.1	14165	30.15	75.38
W2-G-11	1040	1070	220	10	G	1	267	0.83	3.07	0.270	11.9	44.1	8081	36.95	92.38
W2-C-12	1040	1050	220	10	C	1	304	0.94	3.48	0.410	10.6	25.8	8919	36.80	92.0
W2-C-13	1040	1060	220	10	C	1	315	0.97	3.59	0.266	9.8	36.8	17135	38.62	96.6
W2-B-14	1040	1070	218	9	B	1	299	0.92	3.41	0.758	10.5	13.8	8983	17.9	44.8
W2-B-15	1035	1070	218	9	B	1	364	1.12	4.15	0.580	10.4	17.9	9928	2.64	6.36
W2-B-16*	1030	1070	236	18	B	2	433	1.25	4.63	0.760	11.3	14.8	12578	3.54	8.86

Where: w = test panel length; h = test panel height; t = test panel thickness including FRCM; t_f = FRCM thickness; FT = fabric type; NL = number of FRCM layers; G = glass fabric; C = carbon fabric; and B = basalt fabric; P_{max} = maximum diagonal force; υ_{max} = maximum shear stress; ε_y = shear strain at yielding; ε_u = shear strain at failure; μ = pseudo-ductility; T = toughness index; G = modulus of rigidity; E_p = calculated modulus of elasticity; and $\upsilon_{max}/\upsilon_o$ = ratio of shear strength (υ_{max}) to that from as-built tested panel (υ_o).
*double layer of FRCM

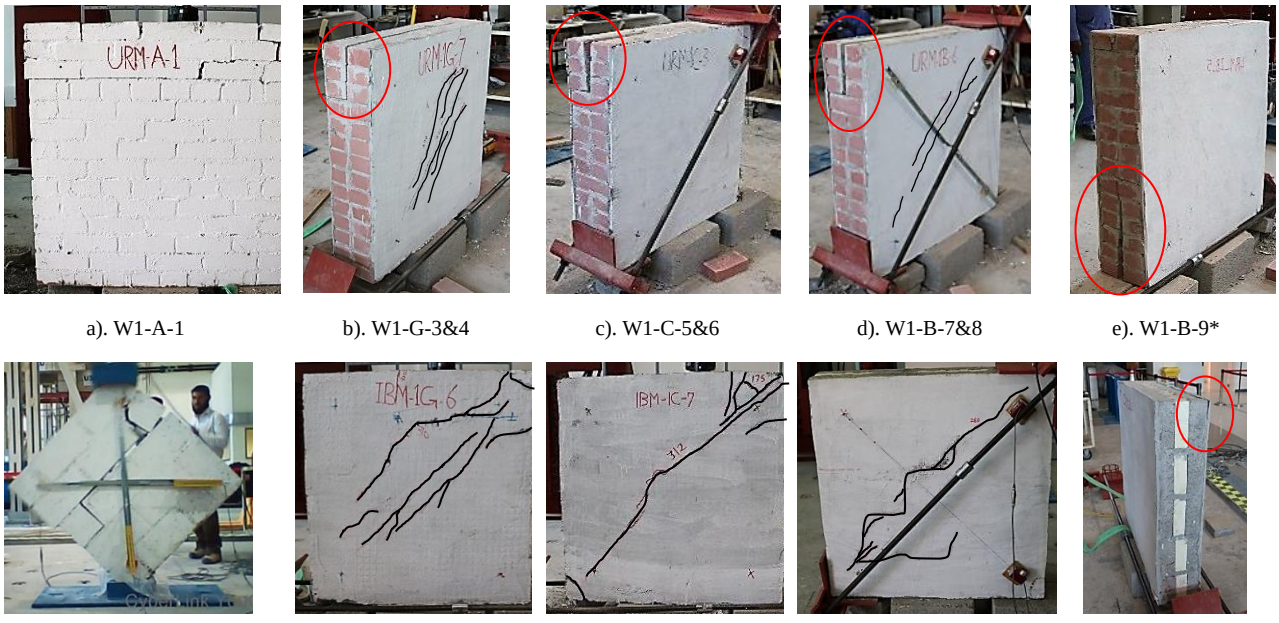

a). W1-A-1 b). W1-G-3&4 c). W1-C-5&6 d). W1-B-7&8 e). W1-B-9*

f). W2-A-2 g). W2-G-10&11 h). W2-C-12&13 i). W2-B-14&15 j). W2-B-16*

Figure 5: Observed crack patterns.

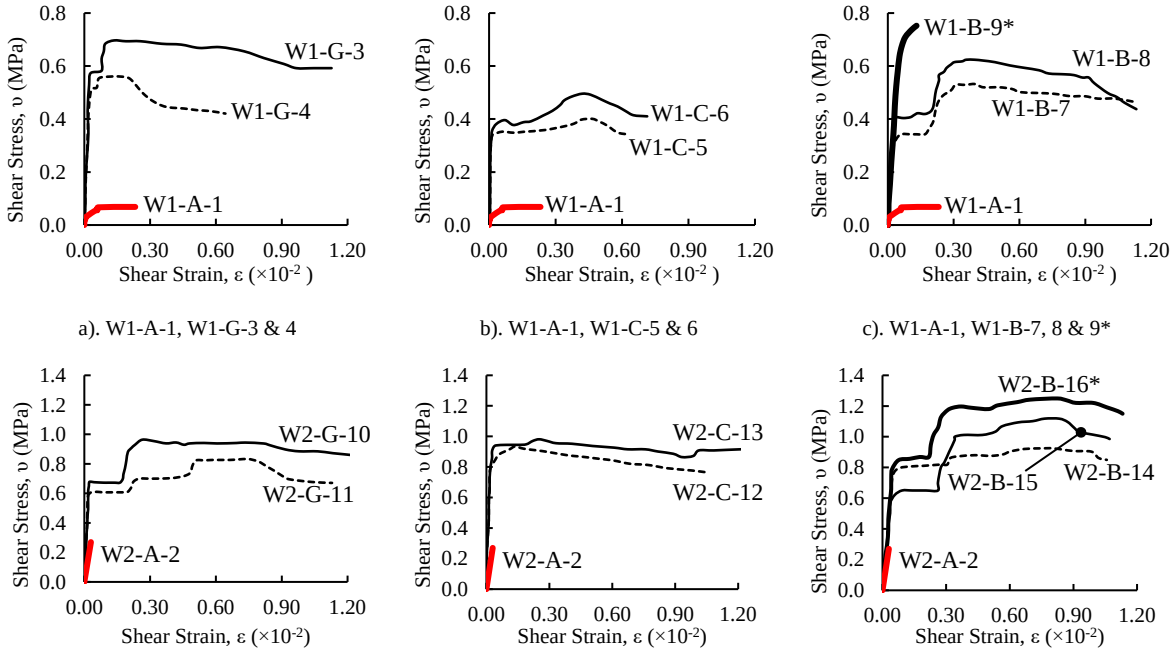

a). W1-A-1, W1-G-3 & 4 b). W1-A-1, W1-C-5 & 6 c). W1-A-1, W1-B-7, 8 & 9*

d). W2-A-2, W2-G-10 & 11 e). W2-A-2, W2-C-12 & 13 f). W2-A-2, W2-B-14, 15 & 16*

Figure 6: Experimental shear stress-strain response.

Failure Patterns and Stress-Strain Behaviour

The as-built tested URM wall (W1-A-1) exhibited a quasi-brittle bed joint sliding shear failure mode and failed at shear stress of 0.10 MPa (see Figure 5a). The failure mode was attributed to mortar reaching its tensile strength (also referred to as modulus of rupture), which is typically very small for vintage URM. Minor localised damage near the loaded corner was also observed, which is attributed to stress concentration.

In the first tested glass FRCM strengthened wall (W1-G-3) localised corner crushing initiated at a shear stress of 0.25 MPa that followed diagonal crack initiation at a shear stress of 0.50 MPa. The test wall failed due to splitting of masonry at unloaded corner at a shear stress of 0.56 MPa (see Figure 5b). Similar damage pattern was observed in the replicate test wall W1-G-4, where the diagonal cracking initiated at 0.56 MPa and splitting of the masonry wythes started at a shear stress of 0.70 MPa.

In test walls strengthened using carbon FRCM (W1-C-5&6) corner damage and diagonal cracks initiated at a shear stress of 0.28 MPa and 0.48 MPa respectively, while the masonry splitting occurred at a shear stress of 0.50 MPa (see Figure 5c). Similar failure mode was also observed in basalt FRCM strengthened test walls (see Figure 5d), where diagonal cracking and some corner crushing led to masonry splitting but at relatively larger shear stress value. The test wall with two layer of basalt FRCM (W1-B-9*) failed due to masonry splitting/crushing at the loaded corner without any signs of diagonal cracking (see Figure 5e).The as-built IMU wall panel (W2-A-1) exhibited brittle failure and collapsed at a shear stress of 0.27 MPa, exhibiting a step joint sliding failure (see Figure 5f). In test walls W2-G-10 and 11, cracking initiated from loaded corners at a shear stress of 0.61 MPa that proceeded towards middle region until a shear stress of 0.95 MPa was reached.

In test walls W2-C-12&13, slight chipping of FRCM at the loaded corner was observed at a shear stress of 0.68 MPa that followed diagonal crack initiation in FRCM at a shear stress of 0.87 MPa (see Figure 5h). Corner crushing started at a shear stress of 0.71 MPa in test walls strengthened using basalt FRCM (W2-B-14&15) and the first diagonal crack appeared at a shear stress of 0.86 MPa that followed a step shaped cracking. Maximum shear stress values recorded in two replicate basalt FRCM strengthened test walls were 0.92 MPa and 1.12 MPa (see Figure 5i). The first corner crack at a shear stress of 1.11 MPa was noted for test wall W2-B-16* and slight FRCM detachment at the loaded corner was also observed at a shear stress value of 1.24 MPa (see Figure 5j) at which point the test was discontinued. Figure 6 shows the experimental stress-strain curves for all test walls.

CONCLUSIONS

Three different types of FRCM systems (basalt, carbon and glass) have been used to strengthen URM and IMU test walls. The strengthened test walls were later tested to investigate the improvement in shear strength, stiffness, and ductility. A total of 16 test walls were subjected to induced diagonal tension in accordance with standardized test procedure. Investigated variables included the masonry type and FRCM fabric type. FRCM were applied on both faces of test walls. Test results were analyzed and crack patterns, stress-strain curves, and values of shear moduli, elastic moduli, pseudo-ductility, toughness, and shear strength were reported. The following are the main conclusions of the experimental program.

1. A brittle failure mode was observed for as-built tested walls, which was similar to that expected. Whereas FRCM strengthened test walls exhibited a relatively ductile failure mode, with failure of URM walls governed by splitting of masonry wythes and failure of IMU characterised by diagonal cracking in FRCM.
2. Shear strength increment due to FRCM strengthening ranged between 422-778% for vintage URM walls and 307-415% for IMU walls when compared to that from as-built tested walls.
3. FRCM fabric rupture or de-bonding from substrate was not observed. It is noted that debonding is the most common failure mode typically reported for epoxy bonded polymer sheets. It may also be inferred that anchors were not

required with FRCM systems tested herein for the application investigated in this study.

4. Splitting/separation of two masonry wythes in URM walls at unloaded corners was attributed to lack of header course and the low tensile strength of the mortar used, which is typically found in vintage buildings.
5. Two layers of basalt FRCM were not very effective in increasing the ductility, however it increased the shear strength of both masonry types minimally.
6. Corner crushing was one of the prominent failure modes observed during testing, which occurred when the stress in corner masonry reached its compression strength. This has been incorporated in guidelines reported in ACI 549.4 by limiting strength of FRCM strengthened masonry walls to toe crushing strength of the strengthened masonry walls.

In general, FRCM was effective in increasing the shear strength and deformation capacity of both types of masonry and thus offers a potentially viable solution to improve the seismic performance of masonry infill walls.

ACKNOWLEDGMENTS

Financial support for this study was provided by the United Arab Emirates University (UAEU) under the research grant G00001603.

REFERENCES

1 Walsh K, Cummuskey P, Jafarzadeh R and Ingham J (2016). "Rapid Identification and Taxonomical Classification of Structural Seismic Attributes in a Regionwide Commercial Building Stock". *Journal of Performance of Construction. Facilities*, **31**(1): 04016067-1,04016067-12.

2 Jiang H, Liu X, and Mao J (2015). "Full-scale experimental study on masonry infilled RC moment-resisting frames under cyclic loads". *Engineering Structures*, **91:** 70-84.

3 Li B, Wang Z, Mosalam KM and Xie H (2008). "Wenchuan earthquake field reconnaissance on reinforced concrete framed buildings with and without masonry infill walls". *Proceedings of the 14th World Conference on Earthquake Engineering* (14WCEE), 12-17 October, Beijing, China.

4 Kam WY, Pampanin S and Elwood K (2011). "Seismic performance of reinforced concrete buildings in the 22 February Christchurch (Lyttleton) earthquake". *Bulletin of the New Zealand Society for Earthquake Engineering*, **44**: 239–278.

5 Ismail N and Khattak N (2016). "Building Typologies Prevalent in Northern Pakistan and their Performance during the 2015 Hindu Kush Earthquake". *Earthquake Spectra*, **32**(4): 2473-2493.

6 Dizhur D, Dhakal RP, Bothara J and Ingham J (2016). "Building typologies and failure modes observed in the 2015 Gorkha (Nepal) earthquake". *Bulletin of the New Zealand Society for Earthquake Engineering*, **49**(2), pp. 211-232.

7 Ismail N, El-Maaddawy T, Najmal A and Khattak N (2017). "Diagonal tension testing of as-built and fabric reinforced cementitious matrix strengthened masonry panels". *Proceedings of the 16th World Conference of Earthquake Engineering* (16WCEE), Chile, South America, 9-13 January, Paper No 4863.

8 Awani O, El-Maaddawy T and Ismail N (2017). "Fabric-reinforced cementitious matrix: A promising strengthening technique for concrete structures". *Construction and Building Materials*, **132**: 94-111.

9 Yardim Y and Lalaj O (2016). "Shear strengthening of unreinforced masonry wall with different fiber reinforced mortar jacketing". *Construction and Building Materials*, **102**: 149-154.

10 Ismail N and Ingham JM (2014). "Polymer textiles as a retrofit material for masonry walls". *Proceedings of the Institution of Civil Engineers - Structures and Buildings*, **167**(1): 15-25.

11 Babaeidarabad S, Arboleda D, Loreto G and Nanni A (2014). "Shear strengthening of un-reinforced concrete masonry walls with fabric-reinforced-cementitious-matrix". *Construction & Building Materials*, **65**: 243-253.

12 Babaeidarabad S, De Caso F and Nanni A (2013). "URM walls strengthened with fabric-reinforced cementitious matrix composite subjected to diagonal compression". *Journal of Composites for Construction*, **18**(2): 04013045.

13 Sagar SL, Singhal V, Rai DC and Gudur P (2017). "Diagonal shear and out-of-plane flexural strength of fabric-reinforced cementitious matrix–strengthened masonry wallets". *Journal of Composites for Construction*, doi: 10.1061/(ASCE)CC.1943-5614.0000796.

14 Lumantarna R, Biggs D and Ingham JM (2013). "Uniaxial compressive strength and stiffness of field-extracted and laboratory-constructed masonry prisms". *Journal of Materials in Civil Engineering*, **26**(4): 567-575.

15 American Society for Testing and Materials International (2003). "*ASTM C270: Standard Test Method for Compressive Strength of Masonry Prisms*". American Society for Testing and Materials International, West Conshohocken, PA, USA.

16 American Society for Testing and Materials International (2008). "*ASTM C109: Standard Test Method for Compressive Strength of Hydraulic Cement Mortars (Using 2-in. or 50-mm Cube Specimens)*". American Society for Testing and Materials International, West Conshohocken, PA, USA.

17 European Committee for Standardization (2004). "*Eurocode 6: Design of Masonry Structures–Part 1–1: Common Rules for Reinforced and Unreinforced Masonry Structures*". ENV 1996-1-1, European Committee for Standardization (CEN), Brussels.

18 Masonry Standards Joint Committee (2011). "*TMS 402: Building Code Requirements for Masonry Structures*". The Masonry Society, Boulder CO.

19 American Concrete Institute (2013). "*ACI 549.4: Guide to Design and Construction of Externally Bonded Fabric-Reinforced Cementitious Matrix (FRCM) Systems for Repair and Strengthening Concrete and Masonry Structures*". American Concrete Institute, USA.

20 American Society for Testing and Materials International (2015). "*ASTM E519: Standard Test Method for Diagonal Tension (Shear) in Masonry Assemblages*". American Society for Testing and Materials International, West Conshohocken, PA, USA.

21 Ismail N., Petersen RB, Masia MJ and Ingham JM (2011). "Diagonal shear behaviour of unreinforced masonry wallettes strengthened using twisted steel bars". *Construction and Building Materials*, **25**(12): 4386-4393.

22 Dizhur D, Griffith M and Ingham JM (2013). "In-plane shear improvement of unreinforced masonry wall panels using NSM CFRP strips". *Journal of Composites for Construction*, **17**(6): 04013010.